Research Article

Saib Thiab Alwan, Abbas Al-Bawee, and Ahmed AAG Alrubaiy*

Behavior of TE and TM propagation modes in nanomaterial graphene using asymmetric slab waveguide

https://doi.org/10.1515/cls-2024-0021
received June 18, 2024; accepted October 23, 2024

Abstract: In this article, the conduction of transverse electric/transverse magnetic (TE/TM) propagation modes in nanomaterial graphene utilization of asymmetric dielectric slab waveguide was studied in terms of their applicability in optical fiber communication. Nano-graphene film was deposited on silica substrate and air cladding. Three layers were exposed to electromagnetic waves with a 1.55 μm wavelength and 1 μm thick nanographene film, silica, and air covering to study the performance and optical properties of graphene nanomaterials. The models were influenced by factors such as attenuation wavenumbers, cut-off frequency, mode number, propagation wavenumbers, skin depth, and angles of total internal reflection. The impact of these parameters was assessed through numerical analysis, revealing significant correlations. The modes generated ten numbers of TE and nine numbers of TM mode dependent upon the structure of nanographene, with low loss propagation wavenumber. As the TE/TM modes increase, the decay wavenumbers of the cladding and substrate parameters diminish. This indicates that the magnetic and electric fields undergo extremely rapid decay beyond the film region, which leads to the skin depth for higher TE/TM modes traveling longer distances in the cladding and substrate than do lower-order modes. Therefore, nanographene exhibits good optical properties due to its low absorption loss. The angles of internal reflection are greater in magnitude than the substrate and cladding key angles. Still, in the tenth TE mode, the internal reflection angles are extremely close to the critical angle as a result of the small substrate decay parameter and the near operating frequency. The tenth TE mode is weakly characterized. The characteristics of TE/TM modes in an asymmetric three-layer slab waveguide structure are realized for various mode orders and various parameters of nanographene material. The field profiles of the TE/TM modes are submitted to comprehend these characteristics.

Keywords: TE/TM modes, waveguide, graphene, microwave propagation, terahertz frequency range, a symmetric dielectric slab

1 Introduction

Numerous studies have examined graphene's potential use in waveguide applications. Graphene is a two-dimensional material with exceptional optical and electronic properties. This review focuses on recent research utilizing asymmetric slab waveguides to investigate the behavior of transverse electric/transverse magnetic (TE/TM) propagation modes in the nanomaterial graphene. Several studies that have contributed to our understanding of this topic are discussed.

Based on a bent asymmetric-slab waveguide, Cao *et al.* [1] proposed an ultra-compact and fabrication-tolerant polarization rotator. A thin layer of graphene was sandwiched between two dielectric layers with varying refractive indices. Shen *et al.* [2] looked at TM modes in a slab waveguide that had a core made of a multilayer structure of graphene and dielectrics and walls made of different common materials. More interestingly, their study found that graphene significantly alters the propagation characteristics of TM modes.

Yang *et al.* [3] examined the transmission characteristics of asymmetric slab waveguides with left-handed materials (LHM). They investigated the transmission characteristics of asymmetric slab waveguides with LHMs and proposed a new dielectric slab waveguide structure with LHM cover and substrate. The researchers discover unusual properties in the asymmetric LHM slab waveguide, such as the absence of fundamental and first-order modes and double degeneracy of higher-order modes. Glytsis [4] offered the basic

* **Corresponding author: Ahmed AAG Alrubaiy,** Department of Materials, College of Engineering, University of Diyala, Diyala, Iraq, e-mail: Ahmed_Ali_eng@uodiyala.edu.iq
Saib Thiab Alwan: Department of Materials, College of Engineering, University of Diyala, Diyala, Iraq, e-mail: Saib_alwan_eng@uodiyala.edu.iq
Abbas Al-Bawee: Department of Materials, College of Engineering, University of Diyala, Diyala, Iraq, e-mail: abbas_taha_eng@uodiyala.edu.iq

concepts of slab dielectric waveguides and elaborated on their significance in optical communication, sensing, and imaging applications.

Using the transfer matrix method, Salman and Yasser [5] analyzed guided modes in a slab waveguide with a central anisotropic metamaterial layer. They showed that mode properties can be controlled by varying the permittivity tensor of the anisotropic metamaterial layer, the metamaterial's thickness, and the refractive index. The study by Taya *et al.* [6] looked at how TE/TM propagation modes work with polarized light in two slab waveguide structures that are made of LHMs and have three layers. The results show that LHM layers have an effect on the confinement factor. To change these parameters, the effective index of TE/TM modes and the thickness of the LHM core layer could be changed. Using double asymmetric discontinuities in leaky wave structures. To prevent open-stopbands, Baccarelli *et al.* [7] presented an innovative approach. The authors demonstrate that high directivity and gain can be obtained with the open stopband effectively blocked by the two asymmetric discontinuities.

In their work, He and Li [8] investigated the differences between graphene waveguides and their TM and TE surface plasmon modes. They found that the TM surface plasmon mode has a higher effective index and a lower confinement factor than the TE surface plasmon mode. The choice of these modes has a significant impact on the waveguides' performance. Raghuwanshi [9] provided an analysis of dielectric optical waveguides to show how the waveguide's structure impacts wave propagation and to what extent it influences the propagation characteristics.

Bai *et al.* [10] explored TE and TM propagation modes in graphene and proposed a TE/TM mode switch using monolayer graphene and metal-dielectric resonances. They demonstrated that the resonant behavior of the device can be modified by adjusting the graphene layer thickness. Liu *et al.* [11] created an efficient and compact TE-TM polarization converter on a silicon-on-insulator platform. Chaharmahali *et al.* [12] focused on controlling terahertz waves using graphene-based metamaterials. They proposed a tunable ultrabroadband terahertz metamaterial absorber and filter using disk graphene patterns, demonstrating their effectiveness for practical applications such as filters and sensors at terahertz spectra.

A study by Evseev *et al.* [13] looked at surface plasmon-polaritons in a symmetric dielectric waveguide with active graphene plates. The results showed that graphene strengthens the connection between plasmons and waves. Kumar *et al.*'s study [14] on metamaterials' impact on evanescent fields in a grounded slab metamaterial waveguide structure showed that metamaterial choice significantly affects the evanescent field. Talebi [15] explored optical modes in slab waveguides and highlighted the significance of the magneto-electric effect in the design of waveguides. Werra *et al.* [16] studied TE resonances in graphene-dielectric structures, noting that the influence of the dielectric layer's thickness and dielectric constant can have a big effect on how the TE mode behaves when it is resonating.

Alwan *et al.* [17,18] studied the impact of polymer thickness and frequency on the TE mode using slab waveguides. They proposed a method for high data rates for optical carriers made of graphene. They showed how the presence of graphene significantly increases the data rate of optical carriers. Graphene modifies the confinement factor and effective index of the TE and TM modes. Controlling these parameters involves adjusting graphene's Fermi energy. The behavior of the TE and TM modes in a silicon nanomaterial slab waveguide was the main focus of the study conducted by Alwan *et al.* [19]. On the TE and TM modes, the silicon nanomaterial layer had a major effect. The ninth TE mode was found to be weakly coupled to the substrate. By adjusting the permittivity tensor of the nanomaterial silicon layer, one could modify the effective index and confinement factor of the TE and TM modes.

1.1 Graphene

Graphene is a versatile material with unique electronic properties due to its hexagonal structure and high mobility of electrical carriers. Its clean manufacturing processes from natural carbon sources make it an environmentally friendly material, enhancing its sustainability in various technological applications. Graphene's superior conductivity makes it ideal for advanced optical communications systems, reducing optical signal loss and improving transmission quality. Its high mechanical strength makes it durable and stable for waveguide structures, ensuring devices can withstand harsh environmental conditions while maintaining high performance. Graphene's high transparency makes it suitable for developing transparent optical devices such as displays, lenses, and sensors. It can also be combined with other materials to enhance properties and expand its use in fields such as medicine, energy, and electronics. Graphene's high thermal stability ensures efficient operation in harsh environments, enhancing device reliability and performance. Its interaction with light opens new possibilities in photonic applications such as communications and optical signal processing [9,10]. Graphene-based waveguides are used in optical interconnects, biosensors, and photonic integrated circuits. Challenges remain in

controlling dispersion and reducing losses in graphene-based waveguides. Overall, the use of graphene in waveguides holds great promise for a vast array of photonics applications especially in polarization controllers in TE or TM mode, where different voltages are applied, making it a valuable material in the design of polarizers [12,20,10].

Graphene has many advantages that make it an ideal material for many applications. Its hexagonal structure and high mobility of electrical carriers give it unique electronic properties. Clean manufacturing processes can produce it from natural carbon sources, making it an environmentally friendly material. This enhances the sustainability of its use in various technological applications. Thanks to its superior and exceptional conductivity, it is an ideal material for use in advanced optical communications systems. It can reduce optical signal loss and improve transmission quality. Its high mechanical strength makes it a durable and stable material for use in waveguide structures. It ensures that devices made from it are able to withstand difficult environmental conditions while maintaining their high performance. Graphene is also characterized by its high transparency, which makes it suitable for developing transparent optical devices such as displays, lenses, and sensors. Innovative applications that require transparent, high-performance materials can use graphene due to this property. Graphene can also be combined with other materials to enhance their properties and expand their use in fields such as medicine, energy, and electronics. In addition, graphene has high thermal stability, which makes it able to work efficiently in harsh environments exposed to high or low temperatures. This thermal stability enhances the reliability and performance of devices made from graphene in various environmental conditions. Graphene can effectively interact with light, opening the door to new possibilities in photonic applications such as communications and optical signal processing. A graphene high-mobility carrier enables efficient, resistance-free electrical conduction.

1.2 Theoretical analysis

A common part used in integrated optics is the three-layer asymmetric dielectric waveguide depicted in (Figure 1) [21].

A thin 2a-thick dielectric film is deposited on a substrate, with a cladding of air above. Total internal reflection propagation occurs when refractive indices $n_f > n_s \geq n_c$ [22].

The expression for the free space wavenumber at the designated operating frequency ω or f in Hertz is by $k_0 = \omega\sqrt{\mu_0 c_0} = 2\pi f/c_0 = 2\pi/\lambda_0$. The fields' t and z dependence is considered to follow the standard exp $j(\omega t - \beta t)$ pattern.

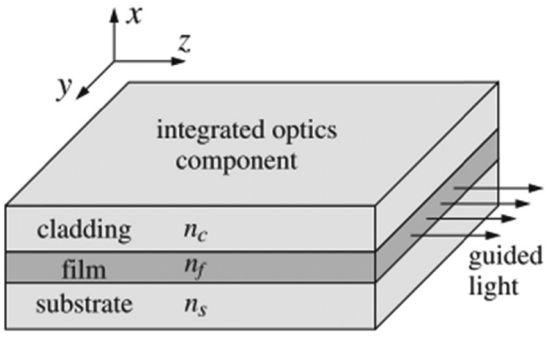

Figure 1: Asymmetric dielectric slab waveguide consisting of three layers.

Adequate positive decay constants (α_s and α_c) are required in both the substrate and cladding to achieve exponential field attenuation with x. Transverse wavenumbers $j\alpha_s$ and $-j\alpha_c$ are corresponding transverse wavenumbers, while real-valued transverse wavenumber k_f within the film is satisfied [23,24]:

$$\begin{aligned} k_f^2 &= k_0^2 n_f^2 - \beta^2 \\ \alpha_s^2 &= \beta^2 - k_0^2 n_s^2 \\ \alpha_c^2 &= \beta^2 - k_0^2 n_c^2 \\ k_f^2 + \alpha_s^2 &= k_0^2 (n_f^2 - n_s^2) \\ \Rightarrow \quad k_f^2 + \alpha_c^2 &= k_0^2 (n_f^2 - n_s^2)(1+\delta) \\ &= k_0^2 (n_f^2 - n_c^2) \\ \alpha_c^2 - \alpha_s^2 &= k_0^2 (n_f^2 - n_s^2)\delta = k_0^2 (n_s^2 - n_c^2), \end{aligned} \tag{1}$$

where a asymmetry parameter δ is

$$\delta = \frac{n_s^2 - n_c^2}{n_f^2 - n_s^2}. \tag{2}$$

The acceptable range of β for guided mode is defined by the inequalities, $k_0 n_s \leq \beta \leq k_0 n_f$, and $\beta \geq k_0 n_c$, assuming that k_f, α_s, and α_c are real.

$$n_c \leq n_s \leq \frac{\beta}{k_0} \leq n_f. \tag{3}$$

1.3 TE modes

The TE modes are initially examined, taking into account the x dependence of the H_z component, which is required in three distinct regions.

$$\begin{aligned} (\partial_x^2 + k_f^2) H_Z \quad (x) &= 0, \ |x| \leq a, \\ (\partial_x^2 - \alpha_c^2) H_Z \quad (x) &= 0, \ x \geq a, \\ (\partial_x^2 - \alpha_s^2) H_Z \quad (x) &= 0, \ x \leq -a. \end{aligned}$$

The solutions, which decrease exponentially, meet the continuity requirements at the boundaries $x = \pm a$:

$$H_Z(x) = \begin{cases} H_1 \sin(k_f x + \phi), & |x| \le a, \\ H_1 \sin(k_f a + \phi) e^{-\alpha_c (x-a)}, & x \ge a, \\ -H_1 \sin \quad (k_f a - \phi) e^{\alpha_s (x+a)}, & x \le -a. \end{cases} \tag{4}$$

The fact that $\mu = \mu_0$ in every area means that E_y is continuous across $x = \pm a$, which means that the H_x components are also continuous, leading to two requirements:

$$\begin{aligned} &\frac{1}{k_f}\cos(k_f a + \phi) = \frac{1}{\alpha_c}\sin(k_f a + \phi) \tan(k_f a + \phi) = \frac{\alpha_c}{k_f}, \\ &\frac{1}{k_f}\cos(k_f a - \phi) = \frac{1}{\alpha_s}\sin(k_f a - \phi) \Rightarrow \tan(k_f a - \phi) = \frac{\alpha_s}{k_f}. \end{aligned} \tag{5}$$

The case of a tangent is uniquely determined up to a multiple of π, which allows us to reverse the roles of two tangents without sacrificing generality:

$$k_f a + \phi = \tan^{-1}\left(\frac{\alpha_c}{k_f}\right) + m\pi,$$

$$k_f a - \phi = \tan^{-1}\left(\frac{\alpha_s}{k_f}\right).$$

The slab's equation and the solution for φ are derived as follows:

$$k_f a = \frac{1}{2} m\pi + \frac{1}{2}\tan^{-1}\left(\frac{\alpha_c}{k_f}\right) + \frac{1}{2}\tan^{-1}\left(\frac{\alpha_c}{k_f}\right), \tag{6}$$

$$\phi = \frac{1}{2} m\pi + \frac{1}{2}\tan^{-1}\left(\frac{\alpha_c}{k_f}\right) - \frac{1}{2}\tan^{-1}\left(\frac{\alpha_s}{k_f}\right). \tag{7}$$

The mth mode is denoted by an integer m, and Eqs. (6) and (1) yield four equations involving the four unknowns $\{\beta, k_f, \alpha_c, \text{and } \alpha_s\}$. The numerical solution is preferred to be in the form of Eq. (6), which introduces dimensionless variables:

$$R = k_0 a\sqrt{n_f^2 - n_s^2} = \frac{2\pi f a}{c_0}\sqrt{n_f^2 - n_s^2} = 2\pi\frac{a}{\lambda_0}\sqrt{n_f^2 - n_s^2}. \tag{8}$$

The propagation constant β, also known as the effective index n_β, can be determined using the following formula:

$$\begin{aligned} \beta &= \sqrt{k_0^2 n_f^2 - k_f^2} \Rightarrow n_\beta = \frac{\beta}{k_0} = \sqrt{n_f^2 - \frac{k_f^2}{k_0^2}} \\ &= \sqrt{n_f^2 - \frac{u^2}{k_0^2 a^2}}. \end{aligned} \tag{9}$$

The objective is to ascertain the quantity of propagating mode and the range of mode indices, as well as the radius R_m of the mth mode.

$$R_m = \frac{1}{2} m\pi + \frac{1}{2}\tan^{-1}(\sqrt{\delta}), m = 0, 1, 2, \ldots. \tag{10}$$

This sets M as the maximum mode index:

$$M = \text{Floor}\left(\frac{2R - \tan^{-1}(\sqrt{\delta})}{\pi}\right). \tag{11}$$

Thus, there are a number of modes ($M + 1$), denote by $m = 0, 1, \ldots, M$, with $\delta = 0$, and the cut-off frequencies found by setting [23]:

$$R_m = \frac{2\pi f_m a}{c_0}\sqrt{n_f^2 - n_s^2} \Rightarrow f_m = \frac{\frac{1}{2} m\pi + \frac{1}{2}\tan^{-1}(\sqrt{\delta})}{\frac{2\pi a}{c_0}\sqrt{n_f^2 - n_s^2}}. \tag{12}$$

1.4 TM modes

In order to derive the TM modes, Eq. (8) are solved separately in each region, followed by the application of boundary conditions, assuming that the modes depend on x-coordinate only, in each region.

$$E_z(x) = \begin{cases} E_1 \sin(k_f x + \phi), & |x| \le a, \\ E_1 \sin(k_f a + \phi) e^{-\alpha_c (x-a)}, & x \ge a, \\ -E_1 \sin(k_f a - \phi) e^{\alpha_s (x+a)}, & x \le -a. \end{cases} \tag{13}$$

The continuity of the normal component of the displacement field $D_x = \epsilon E_x$ across interfaces is a prerequisite for the boundary conditions at $x = \pm a$. This equals tangential field H_y continuity [23]:

$$\begin{aligned} &\frac{\epsilon_f}{k_f}\cos(k_f a + \phi) = \frac{\epsilon_c}{\alpha_c}\sin(k_f a + \phi) \Rightarrow \tan(k_f a + \phi) \\ &\qquad = p_c \frac{\alpha_c}{k_f}, \\ &\frac{\epsilon_f}{k_f}\cos(k_f a - \phi) = \frac{\epsilon_s}{\alpha_s}\sin(k_f a - \phi) = p_s \frac{\alpha_s}{k_f}. \end{aligned} \tag{14}$$

The ratios were defined as follows:

$$p_c = \frac{\epsilon_f}{\epsilon_c} = \frac{n_f^2}{n_c^2}, p_s = \frac{\epsilon_f}{\epsilon_s} = \frac{n_f^2}{n_s^2}. \tag{15}$$

By taking the inverse of the tangents, we can derive the following:

$$k_f a + \phi = \tan^{-1}\left(p_c \frac{\alpha_c}{k_f}\right) + m\pi,$$

$$k_f a - \phi = \tan^{-1}\left(p_s \frac{\alpha_s}{k_f}\right).$$

The slab characteristic equation and φ are determined by the following factors:

$$k_f a = \frac{1}{2}m\pi + \frac{1}{2}\tan^{-1}\left(p_c\frac{\alpha_c}{k_f}\right) + \frac{1}{2}\tan^{-1}\left(p_c\frac{\alpha_c}{k_f}\right), \quad (16)$$

$$\phi = \frac{1}{2}m\pi + \frac{1}{2}\tan^{-1}\left(p_c\frac{\alpha_c}{k_f}\right) - \frac{1}{2}\tan^{-1}\left(p_s\frac{\alpha_s}{k_f}\right). \quad (17)$$

The maximum mode index M is fixed:

$$M = \text{Floor}\left(\frac{2R - \tan^{-1}(p_c\sqrt{\delta})}{\pi}\right), \quad (18)$$

M = 0, 1,..., M denotes the (M + 1) modes, and the cutoff frequencies are established by configuring the following:

$$R_m = \frac{2\pi f_m a}{c_0}\sqrt{n_f^2 - n_s^2} \Rightarrow f_m = \frac{\frac{1}{2}m\pi + \frac{1}{2}\tan^{-1}(p_c\sqrt{\delta})}{\frac{2\pi a}{c_0}\sqrt{n_f^2 - n_s^2}}. \quad (19)$$

The equation $f_m = fR_m/R$, where $f = c_0/\lambda_0$, is used to calculate the total internal reflection angles in the equivalent ray model.

The maximum mode index M, and cut-off frequencies f_m will satisfy inequalities for the TE/TM cases, as pc > 1 [23]:

$$M_{TM} \le M_{TE}, f_{m,TE} \le f_{m,TM}. \quad (20)$$

2 Numerical results and discussion

This section provides an explanation and discussion of the behavior of the TE/TM propagation modes in the MATLAB scripts for nanomaterial graphene. A thin graphene film is applied to silica substrate. On top of the film is a dielectric coating, like air. Graphene nanomaterial was incorporated into an asymmetric slab waveguide in order to assess its optical characteristics and performance. Graphene nanomaterial, with unique characteristics and waveguide parameters such as propagation wavenumbers, modes numbers, cut-off frequencies, decay wavenumbers, transverse wavenumbers, decay wavenumbers, skin depth, and angles of total internal reflection, is utilized in various applications such as asymmetric dielectric slabs, which are the key components of modern integrated optics. The study used an EM wave with a wavelength of 1.55 µm to propagate on a graphene film with a refractive index of 2.75 and a silica substrate with a refractive index of 1.45. The MATLAB application generated both TE/TM modes, with the ten TE modes exhibiting weak binding to the substrate side as a result of a small decay wavenumber and a cutoff frequency that is approaching to the operating frequency.

Figure 3 shows that nine number of TM modes. Note that guide modes within asymmetric slab waveguide include TE/TM modes. The propagation mode (TE) lacks an electric field component in the propagation direction, while the mode (TM) lacks a magnetic field component in the same direction. As a result, TE and TM modes behave similarly, indicating that asymmetric slab waveguides are well suited for efficient and low loss propagation. The transverse profiles for TE and TM modes are plotted in Figures 2 and 3; the

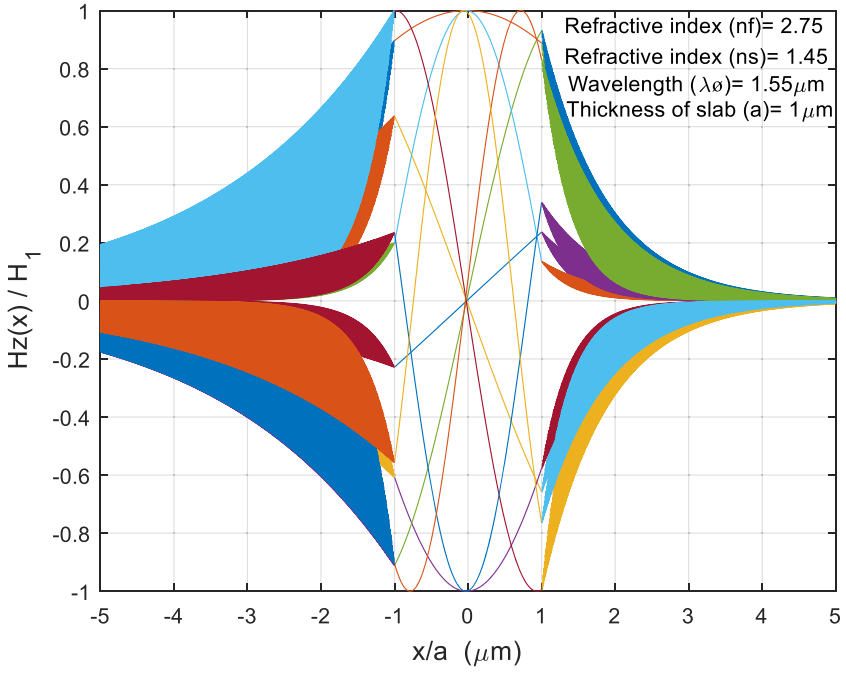

Figure 2: Mode profile for TE modes.

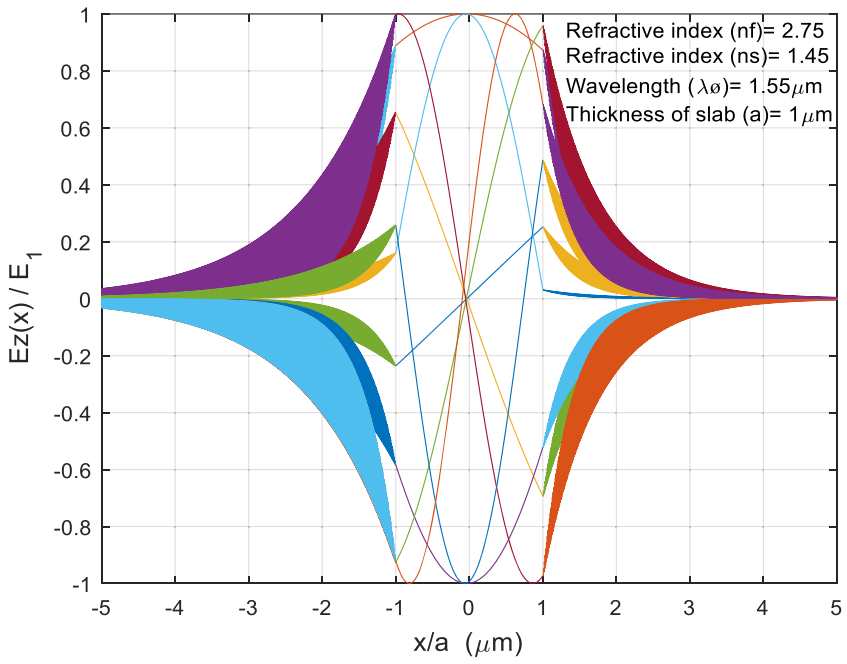

Figure 3: Mode profile for TM modes.

magnetic and electric fields have the typical setup. It oscillates within the slab and becomes evanescent in the surrounding media. The transverse magnetic modes and transverse electric modes are influenced by the structure of graphene, silica substrate, and its refractive indices of substrate and nanomaterial graphene film.

Figure 4 shows the propagation wavenumbers and cut-off frequencies for each TE/TM mode with a constant thickness. The cut-off frequency is directly proportional to the number of TE/TM modes, whereas the propagation wavenumber is inversely proportional. The graphene film thickness and cut-off frequency are fixed for each mode. Higher-order modes propagate with smaller propagation wavenumber values, while lower-order modes propagate with smaller values. The propagation wavenumber is determined by nanomaterial characteristics and wavelengths. A

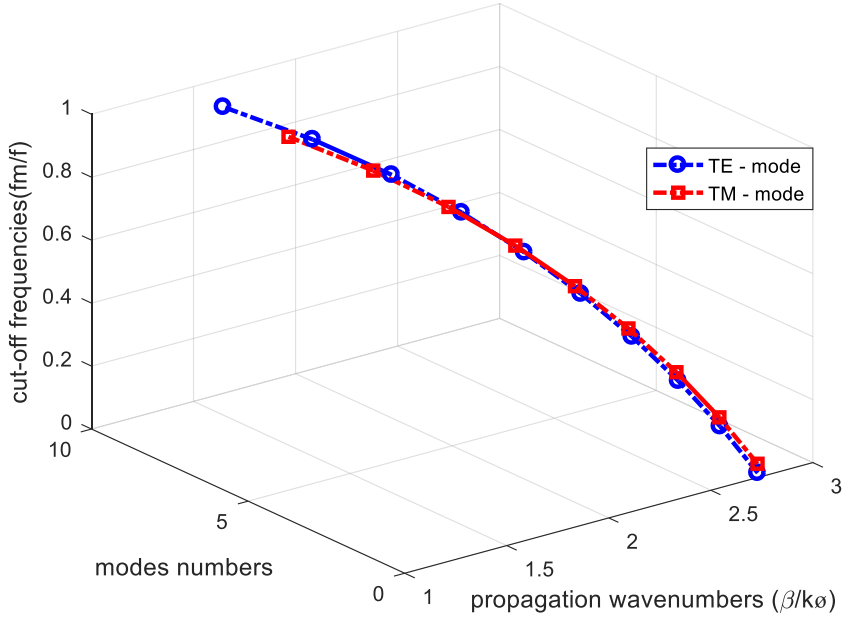

Figure 4: Higher propagation wavenumbers from TE/TM cut-off frequencies in graphene.

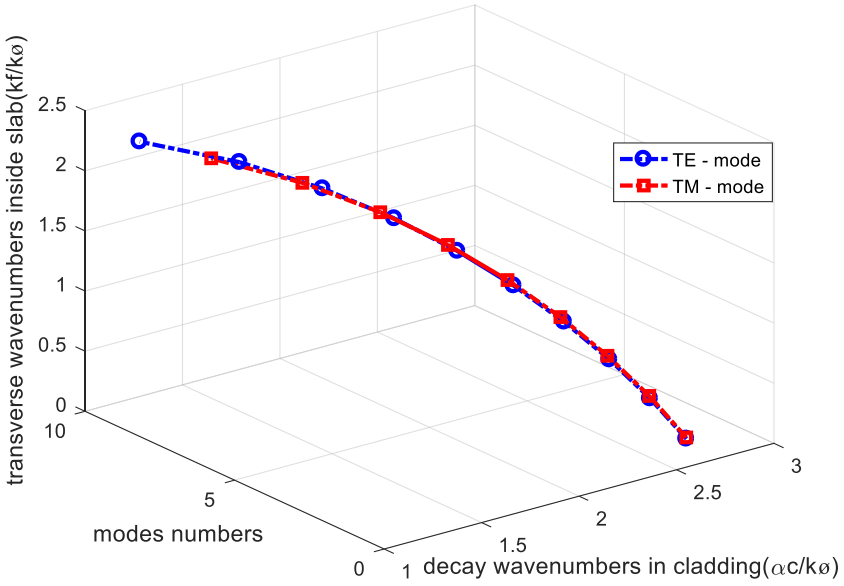

Figure 5: Cladding decay wavenumbers with higher TE/TM modes.

guide TE mode has an equal nearly propagation constant to a TM mode of the same order. The propagation constant has frequency dependence due to the guide's structure and nanomaterial dispersion. Polarization dispersion also exists due to different propagation constants for TE/TM modes.

Electromagnetic waves propagating through graphene nanomaterial attenuate in the direction of propagation. Electric and magnetic fields vary sinusoidally inside the slab, decaying exponentially outside. Upper TE and TM modes have less attenuation wavenumbers than other modes, reducing decay wavenumbers in cladding and substrate parameters as shown in Figures 5 and 6. As wavelength increases, layer decay wavenumbers move to infinite, indicating rapid decay of electric and magnetic fields outside the slab region. This results in a rapid decay of evanescent waves at angles far above the critical angle (21.32°). Transverse wavenumbers within the slab increase in the number of modes, and the cut-off condition occurs when propagation wavenumbers match the transverse wavenumbers inside the slab, resulting in propagation wavenumbers becoming equivalent to those of the surrounding medium.

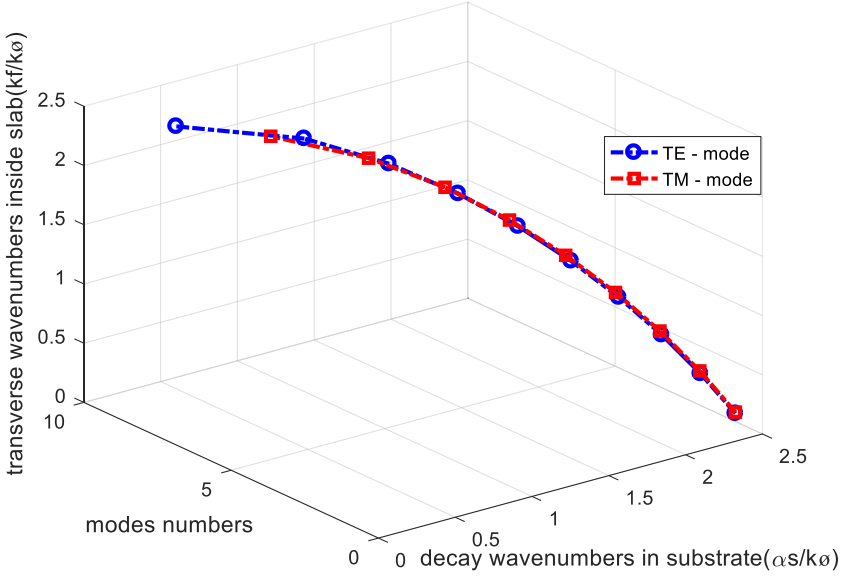

Figure 6: Wavenumbers of substrate decay associated with greater TE/TM modes.

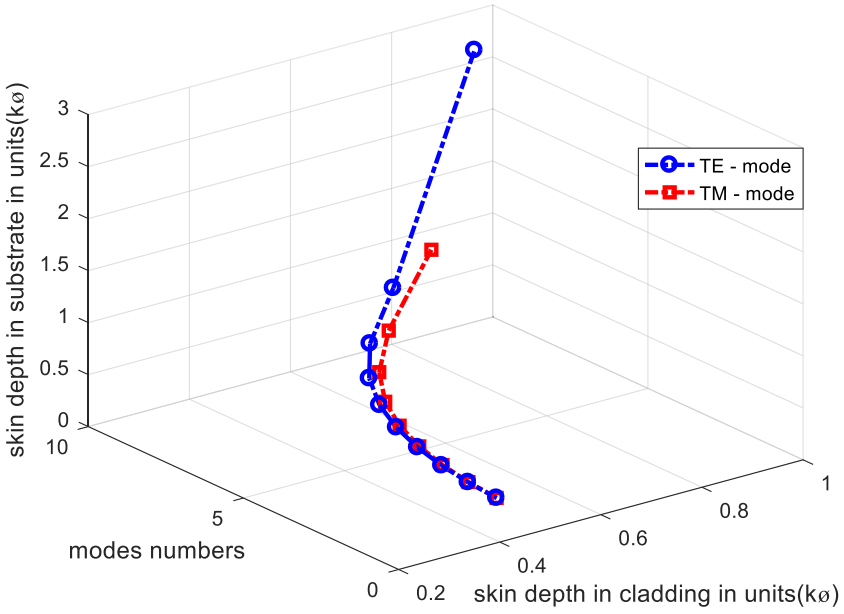

Figure 7: Substrate/cladding skin depth and wavelength-specific TE and TM modes.

Skin depth refers to the decay of electromagnetic waves within graphene nanomaterial. The attenuation wavenumber of the electromagnetic field increases exponentially with the transverse distance, indicating the existence of electromagnetic field within a skin depth, as shown in Figure 7. Increase the number of TE/TM modes also enhances the skin depth in the cladding and substrate at a certain wavelength. Upper TE/TM modes commute longer distances in cladding and substrate than lower-order modes. Therefore, graphene nanomaterials with excellent optical characteristics and low absorption loss are ideal for optoelectronics applications.

The concept involves using asymmetric dielectric slabs for total internal reflection of EM waves. Lossless dielectric slab waveguides experience scattering and absorption due to impurities. Figure 8 illustrates the total internal reflection angles and cut-off radius for the m-th mode at 1.55 μm wavelength and constant graphene thickness. The cut-off

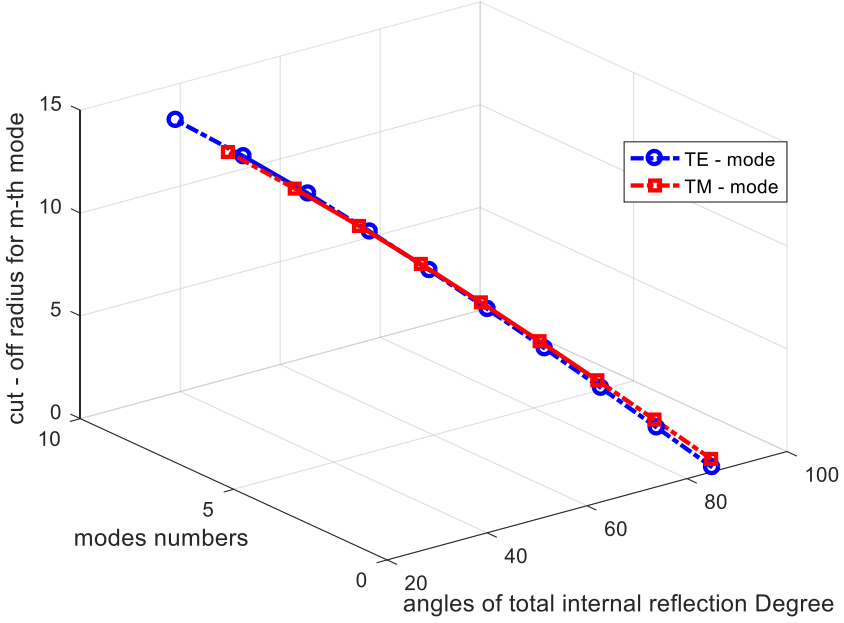

Figure 8: Total internal reflection angles, TE and TM modes, and the mth mode cutoff radius.

radius increases with more TE and TM modes, and internal reflection angles decrease. This means that the increased number of TE/TM modes leads to decreased total internal reflection angles. Higher modes exhibit a bigger cut-off radius and penetrate deeper into graphene nanomaterials. Internal reflection angles exceed critical angles for substrate (31.82°) and cladding (21.32°), except for the tenth TE mode (33.23°). The tenth TE mode's internal reflection angle is near critical due to the small decay parameter and near operating frequency.

Figure 9 displays the angles and wavenumbers for total internal reflection in graphene. It includes TE and TM modes at 1.55 μm wavelength. Figure 9 shows that the number of modes increases with decreasing propagation wavenumbers and the angles of internal reflection decrease. This implies that the angles and propagation wavenumbers reduce with higher modes in graphene nanomaterial. There are two critical angles (31.82°, 21.32°) connected with the internal reflection at the lower and upper interfaces. Critical angles do not depend on EM wave polarization; phase shifts depend on polarization; therefore, it should be noted that the angles of the TE and TM modes in an asymmetric dielectric slab are greater than both critical angles. Consequently, the wave within the slab undergoes total internal reflection at both interfaces and becomes confined within the slab. An asymmetric situation with one cladding close to the slab and another lower than the slab yields the highest slab thickness.

The asymmetric configuration allows one cladding to have a high refractive index, allowing higher modes to escape, while the other cladding can have a low refractive index, enhancing optical confinement. The consequences indicate that the asymmetric slab waveguide may be more advantageous for specific implementations due to its high-power confinement properties in the slab region. Furthermore, the study explores the use of asymmetric planar waveguides in optical fiber communication systems and their potential in wavelength division multiplexing optical networks (WDM).

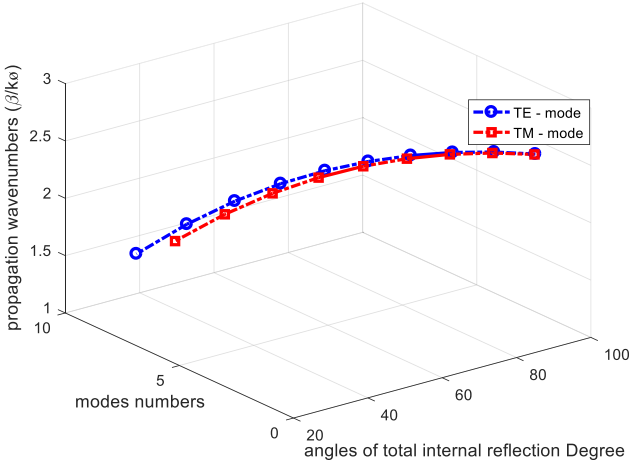

Figure 9: Total internal reflection angles, TE/TM modes, and propagation wavenumbers.

3 Conclusion

The properties of TE/TM modes in an asymmetric three-layer slab waveguide structure were investigated in this study. Note that nanographene is regularly temptingly ascribable to its high non-linear influences and low net absorption in the broad-band optical band; therefore, it is an excellent choice for high rendition, high rapidity, and broad-band optoelectronic and electronic equipment. As an additional result of this effort, field profiles of the TE/TM modes were demonstrated so that the properties of nanographene material for various parameters could be comprehended. The study explores the use of asymmetric planar waveguides in optical fiber communication systems and their potential for WDM optical network applications. Future work will explore various materials with diverse layers to determine their usage, comparing their parameters with standardization to determine the best material for protection and radiation protection.

Funding information: The authors state no funding involved.

Author contributions: All authors have accepted responsibility for the entire content of this manuscript and consented to its submission to the journal, reviewed all the results, and approved the final version of the manuscript. STA conceptualized the study and led the project and developed the model code. AA-B conducted the numerical simulations and data analysis. AAAGA contributed to the development of the theoretical framework and assisted in the interpretation of the results. STA and AAAGA co-wrote the manuscript with input from all authors.

Conflict of interest: The authors state no conflict of interest.

Data availability statement: All data that support the findings of this study are included within the article.

References

[1] Cao T, Chen S, Fei Y, Zhang L, Xu Q-Y. Ultra-compact and fabrication-tolerant polarization rotator based on a bend asymmetric-slab waveguide. Appl Opt. 2013;52(5):990–6.

[2] Shen LF, Xie JP, Wang ZH. Tunable TM modes in a slab waveguide including a graphene-dielectric multilayer structure. Optik (Stuttg). 2021;227:165414.
[3] Yang HW, Dong P, Liu Y. Transmission properties of asymmetric slab waveguides with left-handed materials. J Russian Laser Res. 2009;30:193–203.
[4] Glytsis EN. Introduction to slab dielectric waveguides. Greece: National Technical University of Athens; 2020.
[5] Salman HH, Yasser HA. Guided modes in slab waveguide with central anisotropic metamaterial layer. In IOP Conference Series: Materials Science and Engineering. IOP Publishing; 2020. p. 072127
[6] Taya SA, Jarada AA, Kullab HM. Slab waveguide sensor utilizing left-handed material core and substrate layers. Optik (Stuttg). Oct 2016;127(19):7732–9. doi: 10.1016/j.ijleo.2016.05.095.
[7] Baccarelli P, Burghignoli P, Comite D, Fuscaldo W, Galli A. Open-stopband suppression via double asymmetric discontinuities in 1-D periodic 2-D leaky-wave structures. IEEE Antennas Wirel Propag Lett. 2019;18(10):2066–70.
[8] He XY, Li R. Comparison of graphene-based transverse magnetic and electric surface plasmon modes. IEEE J Sel Top Quantum Electron. 2013;20(1):62–7.
[9] Raghuwanshi SK. Comparative study of asymmetric versus symmetric planar slab dielectric optical waveguides. Indian J Phys. 2010;84:831–46.
[10] Bai T, Tang Y, Hu ZD, Xing T, Lui Z, Huang Y, et al. High-performance sensitive TE/TM mode switch with graphene-based metal-dielectric resonances. IEEE Sens J. 2020;21(3):2791–7.
[11] Liu L, Ding Y, Yvind K, Hvam JM. Efficient and compact TE–TM polarization converter built on silicon-on-insulator platform with a simple fabrication process. Opt Lett. 2011;36(7):1059–61.
[12] Chaharmahali I, Soltani M, Hoseini M, Biabanifard M. Control of terahertz waves for TE and TM modes using graphene-based metamaterials. Opt Eng. 2020;59(4):47101.
[13] Evseev DA, Eliseeva SV, Sementsov DI, Shutyi AM. A surface plasmon–polariton in a symmetric dielectric waveguide with active graphene plates. Photonics. 2022;9:587.
[14] Kumar S, Kumari A, Pradhan B. Analysis of evanescent field of TE and TM mode in the grounded slab metamaterial waveguide structure. Opt (Stuttg). 2015;126(23):3706–12.
[15] Talebi N. Optical modes in slab waveguides with magnetoelectric effect. J Opt. 2016;18(5):055607.
[16] Werra JFM, Intravaia F, Busch K. TE resonances in graphene-dielectric structures. J Opt. 2016;18(3):034001.
[17] Alwan ST, Mahmood OA, Mahmood T. Generate high data rate of optical carries by using nanomaterial graphene in slab waveguide. Curved Layer Struct. 2022;9(1):187–92.
[18] Alwan ST, Mohamed WQ, Mahmood H. Effects of polymer thickness and frequency on the TE-mode using slab waveguide. 2019 3rd International Symposium on Multidisciplinary Studies and Innovative Technologies (ISMSIT). IEEE; 2019. p. 1–10.
[19] Alwan ST, Jasim AN, Mahmood T, Al-Rubaiy AAAG. Propagation modes of TE and TM properties in nanomaterial silicon by using asymmetric slab waveguide. 2023 3rd International Scientific Conference of Engineering Sciences (ISCES). IEEE; May 2023. p. 128–33. doi: 10.1109/ISCES58193.2023.10311451.
[20] Song X, Dai X, Xiang Y. Graphene based waveguides. In Emerging waveguide technology. Vol. 131. London: InTechOpen; 2018.
[21] Doerr CR, Kogelnik H. Dielectric waveguide theory. J Lightwave Technol. 2008;26(9):1176–87.
[22] Kong L, Wang C, Yin X, Fan X, Wang W, Huang J. Electromagnetic wave absorption properties of a carbon nanotube modified by a tetrapyridinoporphyrazine interface layer. J Mater Chem C Mater. 2017;5(30):7479–88.
[23] Orfanidis SJ. Electromagnetic waves and antennas. 2016. [Online] Available: http://eceweb1.rutgers.edu/%7eorfanidi/ewa/.
[24] Lotspeich JF. Explicit general eigenvalue solutions for dielectric slab waveguides. Appl Opt. 1975;14(2):327–35.